

Research paper

# Evaluation of the powering extrapolation of a ship with a gate rudder system, including ageing and fouling effects

Çağatay Sabri Köksal<sup>a,\*</sup>, Cihad Çelik<sup>b</sup>, Selahattin Özsayan<sup>b</sup>, Emin Korkut<sup>b</sup>, Mehmet Atlar<sup>a</sup>

<sup>a</sup> Naval Architecture, Ocean and Marine Engineering, University of Strathclyde, Glasgow, United Kingdom

<sup>b</sup> Faculty of Naval Architecture and Ocean Engineering, Istanbul Technical University, Istanbul, Turkey

## ARTICLE INFO

## Keywords:

Gate rudder system  
Sea trials  
Ship model test  
Ageing and fouling effect

## ABSTRACT

This paper is based on the evaluation results of the calm water powering extrapolation of a 90-m general cargo vessel, originally built with a conventional rudder system (CRS) and later retrofitted with an innovative energy-saving device (ESD) known as the Gate Rudder System® (GRS), as part of the EU H2020 Project GATERS. The power estimation of the vessel was conducted using an adapted extrapolation procedure based on the scaled model tests of the vessel in a towing tank, validated by the three sets of sea trials. The first sea trial was performed when the ship was new, while the latter two were conducted during the project timeline, before and after the GRS retrofit. This paper aims to adapt the ITTC-78 power extrapolation method to predict the power performance of a ship retrofitted with the GRS for the first time in the maritime industry. Within this framework, the specific objectives of the paper are to describe and validate the proposed method using relevant power-speed data of the GATERS project target vessel (M/V ERGE) initially equipped with the CRS and later replaced by the retrofit GRS to achieve the project objective. Due to the real-world circumstances of retrofitting a 13-year-old ship with a novel energy-saving device, investigating the effects of ageing, hull roughness, and fouling has also become one of the key objectives of the paper. The findings demonstrate the ageing effect on the target ship's powering performance after retrofitting with GRS, highlighting the need for special consideration of power extrapolation alongside the hull fouling effects. The paper also demonstrates that the GRS is an emerging ESD, as a retrofit beside newly built ships with GRS, which improved the powering performance of the project target vessel, achieving a remarkable 25% power saving based on the comparative full-scale sea trials.

## Nomenclature

$C_A$	Correlation allowance	$n$	Propeller rate of revolution
$C_{AA}$	Air resistance coefficient	$N_P$	Number of propellers
$C_F$	Frictional resistance coefficient	$P_E$	Effective power
$C_R$	Residual resistance coefficient	$R_e$	Reynolds number
$C_T$	Total resistance coefficient	$S$	Wetted surface
$F_D$	Skin friction correction	$t$	Thrust deduction factor
$J$	Propeller advance coefficient	$V$	Ship speed
$k$	Form factor	$w$	Taylor wake fraction
$K_Q$	Propeller torque coefficient	$\Delta C_F$	Roughness allowance
$k_s$	Roughness of hull surface	$\eta_0$	Propeller open water efficiency
$K_T$	Propeller thrust coefficient	$\rho$	Water density in general

## 1. Introduction

The International Maritime Organization (IMO) has set a number of regulations to reduce the carbon emissions of ships which can be newly built or existing. Ship owners must comply with the Energy Efficiency Design Index (EEDI) for ships to be built and the Energy Efficiency Existing Ship Index (EEXI) for already built ships, amongst other criteria. The major requirement of these two criteria is to improve the vessel's efficiency, which implies a reduction in power demand. One potential solution for reducing ships' power requirements and, consequently, their carbon footprint is to use energy-saving devices (ESD). Among these devices, the Gate Rudder System (GRS) stands out, as it can be effectively retrofitted to existing ships or installed on newly designed vessels. It also presents attractive energy savings with double figures (Tacar et al., 2020) compared to ships with conventional rudder systems (CRS). Ships with GRS can have several advantages over ships with CRS

\* Corresponding author.

E-mail address: [cagatay.koksal@strath.ac.uk](mailto:cagatay.koksal@strath.ac.uk) (Ç.S. Köksal).

<https://doi.org/10.1016/j.oceaneng.2024.119503>

Received 28 May 2024; Received in revised form 10 October 2024; Accepted 11 October 2024

Available online 22 October 2024

0029-8018/© 2024 The Authors. Published by Elsevier Ltd. This is an open access article under the CC BY license (<http://creativecommons.org/licenses/by/4.0/>).

in terms of propulsive efficiency, seakeeping, and manoeuvrability. The GRS works as an accelerating duct; hence, the rudder blades generate thrust, while a favourable propeller-rudder-hull interaction further improves the propulsive efficiency. The twin rudder blades, each located aside from the propeller, can be controlled individually during sailing, hence enhancing ships' manoeuvring performance, especially in harbours at zero and slow speeds. This is in addition to typically much smaller overshoot angles compared to ships with CRS during zig-zag tests [Carchen et al. \(2021\)](#). As the first-ever full-scale application of the GRS, the comparative sea trials of the two 2400 GT sister container vessels, SAKURA ([Fukazawa et al., 2018](#)) appended with the conventional rudder system (CRS), and SHIGENOBU ([Sasaki et al., 2019](#)) with the Gate Rudder System demonstrated a 14% energy saving for the favour of the latter with the GRS. In Japan, the model scale investigations were carried out experimentally and numerically on a large bulk carrier, and the GRS-fitted model projected a fuel saving of up to 7–8% in the powering analysis. It is well known that conventional ducted propellers may have disadvantages in terms of cavitation and vibration. There are also available studies that focus on cavitation and vibration problems comparing the CRS and GRS configurations. Numerical and experimental studies reported that sheet and tip-vortex cavitation could be reduced with the GRS-fitted ships. One further full-scale testimony from SHIGENOBU's captain was that the GRS resulted in less vibration and quieter aft accommodation areas.

In recent years, both experimental and numerical studies have been conducted to investigate the effects of the GRS on various aspects, including ship powering performance, seakeeping, manoeuvrability, propeller cavitation, and underwater radiated noise (URN). Many of these studies have specifically focused on enhancing powering performance and achieving energy savings in ships. [Turkmen et al. \(2015\)](#) carried out a series of tests in the Emerson Cavitation Tunnel (ECT) and measured and compared the forces on the GRS and CRS behind the ship. All of these measurements were conducted at the model scale, and the open-water data for the propeller with GRS around it were obtained from these open-water tests. The measurements show that the GRS rudder blades generate additional thrust with the increased rotational rate of the propeller, while the conventional rudder generates additional frictional force. [Turkmen et al. \(2015\)](#) found a 4–8% higher effective thrust factor (1-t) (or smaller thrust deduction factor, t) in propulsion tests with GRS compared to CRS. Also, in the comparative analysis of the open water data for a propeller with a gate rudder and a conventional rudder, a 15–25% higher wake factor (1-w) (or lower effective wake fraction, w) value was obtained with the GRS. [Turkmen et al. \(2015\)](#) also investigated the effect of full-scale GRS on the aft end flow field by CFD analysis. It was observed that when the gate rudder was placed closer to the propeller plane (at  $1.25 \times R$  compared to  $1.50 \times R$ ), there was a 10% increase in thrust force. [Sasaki et al. \(2016\)](#) conducted an experimental and computational study on the application of the GRS for a large bulk carrier. The forces on the gate rudder were measured, and it was shown that the GRS presented a thrust of 6% of the hull resistance. The study indicated that the gate rudder provides an energy saving of 7–8% and would amortise the investment cost within 0.37–0.9 years. In the recently completed EU-H2020 project [GATERS \(2021\)](#), [Köksal et al. \(2022\)](#) and [Köksal et al. \(2024a\)](#) examined the results of the resistance, propulsion, and seakeeping experiments conducted with the GATERS target ship (M/V ERGE) model at the Kelvin Hydrodynamics Laboratory (KHL) of the University of Strathclyde. In the calm water resistance experiment, the model with GRS reduced the hull resistance by 4% compared to the model with CRS. In the propulsion test, the GRS improved the delivered power by over 10% compared to the hull with CRS. Seakeeping tests were conducted in regular waves to simulate oblique wave conditions. A comparison of the powering performance of the vessel with the CRS and GRS revealed that torque was 20% less for the GRS than that in the model the CRS. [Çelik et al. \(2022\)](#) extrapolated the model test results for 2400 TEU Containership obtained from the Ata Nutku Ship Model Testing Laboratory's towing tank of Istanbul

Technical University to full scale using various methods. Comparing these extrapolated results with the sea trials data, the method where the GRS was considered as an appendage showed better agreement. The powering predictions indicated that the GRS configuration could reduce the power requirement by 2% at the design speed compared to the CRS configuration under full-loaded conditions. As part of the GATERS project investigations, [Mizzi et al. \(2022\)](#) demonstrated the assessment of CFD methods, solvers, and approaches used to accurately predict the performance of ships with GRS. Specifically, simulations at the model scale were conducted for the M/V ERGE ship using two different turbulence models, and the obtained results were validated with experimental data.

In addition to the investigations in the GATERS project, research related to the GRS has been expanded through full-scale sea trial tests conducted on multiple ships. [Sasaki et al. \(2019\)](#) shared the sea trial results of two 2400 DWT sister container ships, one equipped with the GRS for the first time (SHIGENOBU) and the other with a conventional rudder (SAKURA), and examined the extrapolation method for the powering estimations from model to full scale. When the sea trial results were examined comparatively, the GRS provided a 14% reduction in fuel consumption compared to the CRS. Furthermore, it was seen that the utilisation of the GRS could lead to a service performance improvement of this vessel by up to 30% in rough seas. It was stated that using the conventional rudder approach in the powering procedure will not give accurate results, especially in the value of effective wake fraction. [Sasaki and Atlar \(2018\)](#) conducted a comparative analysis of the propulsive efficiency characteristics (thrust deduction and effective wake fraction) of a ship with GRS in comparison with a ship with CRS by model tests, CFD results, and sea trial data from two container vessels. As a result of these investigations, it was demonstrated that the thrust deduction (t) of the GRS is expected to be lower compared to the conventional rudder system, while the effective wake fraction is expected to be larger. [Tacar et al. \(2020\)](#) conducted an experimental and numerical study to investigate the effect on ship performance of a container ship equipped with GRS for full and trial load. Experimental and numerical studies were carried out with models of 2 m and 5 m, and the scale effect was examined. [Tacar et al. \(2020\)](#) demonstrated that as the speed of the vessel increased, the advantageous effect of the GRS became more pronounced compared to the CRS at the trial conditions. Furthermore, they highlighted that at a service speed of 15 knots, the ship equipped with the GRS required approximately 17% less brake power compared to the one fitted with a CRS. The authors found that concerning scale effects, the smaller model tends to overpredict, whereas the larger model tends to underpredict the power requirement when compared to sea trial measurements. [Çelik et al. \(2023\)](#) analysed the results of three different sea trials data for the M/V ERGE ship to examine the accuracy of extrapolating model test measurements to full scale. Additional frictional resistance due to ageing and fouling effects was included in the full-scale extrapolation, and the results were compared with those of the sea trial. The analysis revealed that during the January 2023 trials, M/V ERGE experienced a 21% increase in power with the CRS at a speed of 11.5 knots due to ageing and fouling conditions.

On the other hand, the optimisation studies for improving the powering performance of the GRS were presented in [Gürkan et al. \(2023a\)](#), [Gürkan et al. \(2023b\)](#), and [Gürkan et al. \(2023c\)](#) within the framework of the GATERS project. In addition to these studies on powering performance and energy efficiency, there has also been a focus on investigating the effects of the GRS on manoeuvrability. [Sasaki et al. \(2017\)](#), [Fukazawa et al. \(2018\)](#), [Carchen et al. \(2021\)](#), and [Gürkan et al. \(2023d\)](#) presented their studies involving various aspects of manoeuvrings of the ships with GRS. [Turkmen et al. \(2018\)](#), [Özsayan et al. \(2023\)](#), [Santic et al. \(2023\)](#), [Köksal et al. \(2023a\)](#), [Köksal et al. \(2023b\)](#), [Özsayan et al. \(2024\)](#), [Köksal et al. \(2023c\)](#) and [Köksal et al. \(2024b\)](#) also conducted experimental and numerical investigations involving the cavitation, URN and detailed flow analyses of ships with the GRS.

Recently, [Sasaki and Atlar \(2024\)](#) claimed that GRS could offer significant design advantages and, hence, the development of new hull forms, which could be more advantageous. Their study introduced four applications emphasising, namely, (i) how GRS-equipped ships could eliminate the higher CAPEX cost of GRS with savings in hull steel weight; (ii) being complementary for vessels to be fitted with WASP (wind-assisted ship propulsion) in providing effective counterbalancing heel/yawing moments; (iii) presenting reduced URN and; (iv) offering potentially the best solution for resolving the contradiction between EEDI 'Phase 3' and MPP requirements. [Bulten \(2024\)](#) conducted full-scale CFD studies of a bulk carrier equipped with the GRS and also examined scenarios expected to arise when this ship is equipped with a WASP. To cover a broader operating range, a dynamic system simulation model based on the CFD dataset was developed. This model provides ship operating conditions (such as ship speed and external forces) to encompass a broader range of operational scenarios.

This paper is based on the evaluation results of the calm water powering extrapolation of the 90 m general cargo vessel M/V ERGE, which was originally built with the CRS but later was retrofitted with the GRS as the main objective of the EU H2020 Innovation Action project, [GATERS \(2021\)](#), [Atlar et al. \(2023\)](#). M/V ERGE was used as the project target vessel to demonstrate the viability of the GRS as a retrofit on a commercial coastal vessel, which was one of the main objectives of this project. Within the GATERS project, the powering estimation of M/V ERGE was conducted using a suitable extrapolation procedure based on the scaled model tests of M/V ERGE in a towing tank. Also, three sets of sea trials of M/V ERGE were conducted. The first trials were conducted with the new ship with CRS in 2010, while the latter two trials were conducted in 2023 during the GATERS project and before and after the GRS was retrofitted in January 2023 and May 2023, respectively. The main objective of the latter two trials was to demonstrate the effectiveness of the GRS as well as to support other objectives of the project, including the validation of the powering extrapolation and numerical prediction methods.

The present paper discusses the comparative evaluation results of the powering predictions of M/V ERGE before and after the retrofit of GRS to demonstrate its effectiveness as a novel, attractive and emerging energy-saving device for ships. Since the evaluation study involves the retrofit of an existing ship, which is 13 years old, issues such as ageing and fouling effects will play an essential role during the extrapolation procedure. The study, therefore, not only demonstrates the effectiveness of the novel energy-saving device, the GRS, on an existing ship based on the full-scale sea trials for the first time, but it also studies the complex combined effects of the ageing and fouling effects, including the laborious and scarce underwater hull roughness and fouling surveys, and roughness measurements taken just before and after the ship's drydock. Therefore, the novel contributions distinguishing the current study from the already reported investigations are (a) Providing the full-scale performance data of a commercial and its analysis for the novel GRS for the first time as a retrofit in the literature; (b) An accurate assessment of the complex ageing and fouling effects through the full-scale roughness and fouling data measurements and analyses. The analysis method of the data for the latter (b) may not be novel, but the analysed performance data for the GRS is clearly unique and non-existent. The analysis was conducted using full-scale data collected in real-world conditions, which was never published before for a retrofit GRS. Moreover, it is unrealistic to achieve an ideal environment where all variables align as expected. A reliable powering performance analysis may require comparing sister ships with differing hull surface conditions, ages, and other factors where the practical approach proposed in this study will be most appropriate. In the [GATERS \(2021\)](#) project, the target ship, built in 2010 with CRS, was retrofitted with GRS in 2023. As a result, it was not feasible to restore the hull surface to conditions comparable to those of CRS and GRS, complicating an accurate comparison of the GRS's effect between the two systems due to ageing and fouling effects.

In addition to the above-described circumstances, the original plan for the sea trials with CRS was to drydock the vessel, clean the hull, and conduct the trials under 'as clean' conditions. However, this could not be achieved due to an overbooked drydocking schedule caused by the backlog of COVID-19-related ship maintenance activities. Even if hull cleaning had been possible, a fair comparison would still not have been achievable, given that the hull was 13 years old and the effects of ageing would still need to be considered. Hence, the study presents the performance results of the first retrofit application of the GRS with an emphasis on the hull roughness and fouling during the powering performance analysis. In this respect, an up-to-date literature review focused on GRS technology is provided. The methodology for the hull roughness survey, as well as the details of the underwater and drydock fouling surveys, are explained. A summary of the sea trials, including the hull conditions observed, is provided. The discussions are expanded to draw conclusions on the additional frictional resistance caused by ageing and fouling effects.

Based on the above background, the aim of the study is to evaluate the accuracy of the vessel's performance predictions based on model tests and sea trials in terms of the assumption made regarding the roughness allowance, which relies on hull roughness measurements and fouling conditions, to assess the effectiveness of the GRS. The assessment of hull roughness and fouling is necessary because the vessel is affected by ageing, and an accurate evaluation of the first retrofit application of such a novel concept is noteworthy. The reference sea trials of the vessel with the CRS correspond to the period of the vessel's construction and just before the GRS retrofit. Therefore, it is essential to evaluate all factors, including the results of model tests, sea trials, roughness measurements, and fouling surveys, to draw a solid conclusion on the effectiveness of the GRS compared to the CRS. Following this introductory section, the details of the towing tank tests with M/V ERGE's scaled model, testing facility, procedures and test cases are presented in Section 2. This is followed by the details of the sea trials, including the evaluation of ageing and fouling effect in Section 3. The results and discussions of the study are presented in Section 4, followed by the concluding remarks in Section 5.

## 2. Towing tank tests

### 2.1. Test setup

A wooden model ([Fig. 1](#)) with a scale of 1/23.7 of the target vessel M/V ERGE was built following the ITTC procedure ([ITTC, 2017a](#)) that is typically used in the resistance and propulsion tests in Istanbul Technical University's Ata Nutku Ship Model Testing Laboratory. The towing tank has the dimensions of  $160 \times 6 \times 3.4$  (L  $\times$  B  $\times$  H) m, and the maximum carriage speed is up to 5.5 m/s. The ship model was free to trim and sink during the resistance and propulsion tests. A custom-made measurement system was manufactured to accurately measure forces and moments acting on both rudder blades ([Fig. 1](#)), as well as to adjust the rudder blade angles ([Fig. 2](#)). The geometric features of the M/V ERGE and its model are given in [Table 1](#).

A stock propeller model was used during the experiments for both configurations (i.e., with CRS and GRS). The model propeller was a fixed pitch, right-handed and four-bladed one, as shown in ([Fig. 2 d](#)) and with the geometric features given in [Table 2](#).

### 2.2. Test procedure

The Ata Nutku Ship Model Testing Laboratory towing tank ( $160 \times 6 \times 3.4$ ) is equipped with a manned carriage and a computer-controlled flap-based wave-maker that has the capacity to generate regular and irregular waves. There is a beach for absorbing the waves and reducing wave reflections at the opposite end of the wave-maker. In the context of self-propulsion tests, it is necessary to consider an additional towing force to determine the full-scale ship's propulsion characteristics

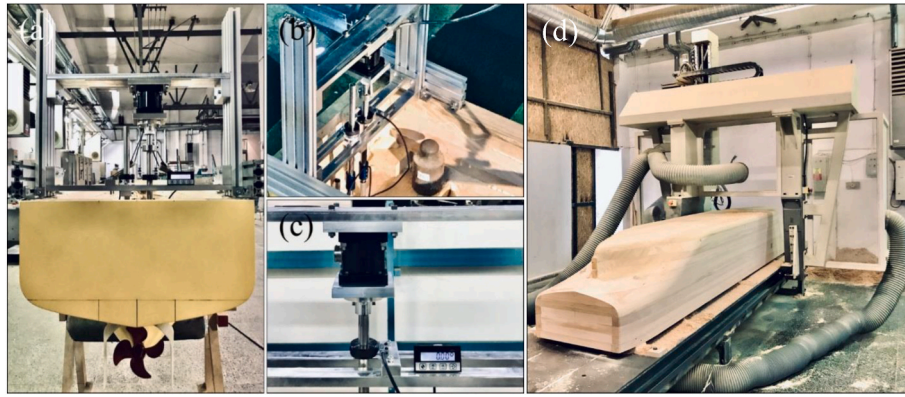


Fig. 1. (a) Stern view of the ship model, (b) and (c) custom-made measurement system, (d) model construction phase.

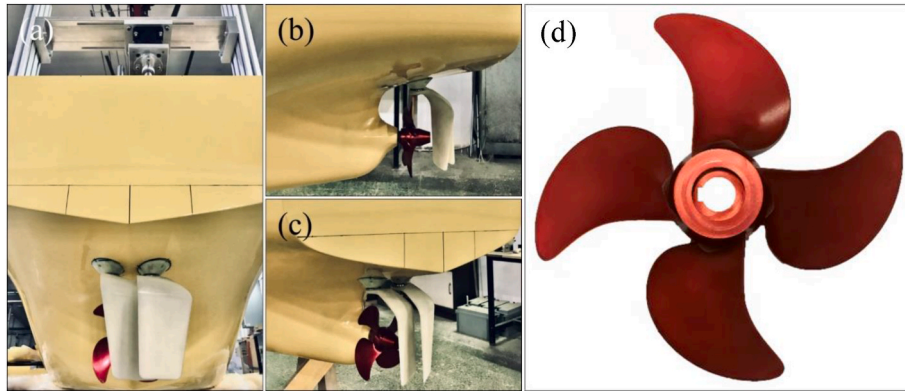


Fig. 2. (a) Back, (b) port-side and (c) general view of the stern with the GRS. (d) Model propeller.

**Table 1**  
Actual ship (M/V ERGE) and its model characteristics.

Parameters	Symbol	Ship	Model
Scale	$\lambda$	1	23.70
Length between PPs (m)	$L_{PP}$	84.95	3.584
Breadth at WL (m)	$B_{WL}$	15.40	0.650
Draught (midship) (m)	$T$	3.300	0.139
Propeller diameter (m)	$D_p$	3.600	0.152

**Table 2**  
Model propeller characteristics.

Parameters	Symbol	Value
Diameter	$D$	0.152
Chord length (r/R:0.7)	$c_{0.7}$	0.050
Pitch ratio (r/R: 0.7)	$P_{0.7}/D$	0.835
Blade area ratio	$A_E/A_0$	0.512
Hub ratio	$d_h/D$	0.250

accurately. This external force, denoted as  $F_D$ , commonly referred to as the Skin Friction Correction (SFC), to compensate for variation in the Reynolds numbers ( $Re$ ) between the model and the full-scale ship. The calculation of  $F_D$  is outlined in Eq. (1), following the guidelines given by ITTC (2017b).

$$F_D = \frac{1}{2} \rho S V^2 [(1+k)(C_{FS} - C_{FM}) - \Delta C_F] \quad (1)$$

The performance characteristics of the full-scale propeller were calculated from the model propeller characteristics in open water, which were corrected for the scale effect according to the 1978 ITTC performance prediction procedure (ITTC, 2017c). The load of the full-scale propeller is obtained from:

$$\frac{K_{TS}}{J_s^2} = \frac{1}{N_p} \frac{S_s}{2D_s^2} \frac{C_T}{(1-t)(1-w_{TS})^2} \quad (2)$$

with this,  $K_T/J^2$  as the input value, the full-scale advance coefficient  $J_{TS}$  and torque coefficient  $K_{QTS}$  are read off from the full-scale propeller characteristics, and further performance data were calculated as follows.

The propeller rate of revolutions ( $n_s$ ) is

$$n_s = \frac{(1-w_s)v}{J_{TS}D_s} \quad (3)$$

and the thrust of the propeller ( $T_s$ ) is

$$T_s = \frac{K_T}{J^2} J_{TS}^2 \rho_s D_s^4 n_s^2 \quad (4)$$

the torque of the propeller ( $Q_s$ ) is

$$Q_s = \frac{K_{QTS}}{\eta_R} \rho_s D_s^5 n_s^2 \quad (5)$$

the delivered power ( $P_D$ ) is

$$P_D = 2\pi Q_s n_s \quad (6)$$

In the analysis of the ship with the CRS, the model wake fraction was converted to the full-scale wake fraction using the standard procedure (ITTC 2017c). However, the extrapolation of the model wake fraction to full-scale used the below approach (Eq. (7)) based on the accumulated knowledge of the previous ships with GRS and CRS (Sasaki, 2022).

$$w_M = w_S \quad (7)$$

### 3. Sea trials

M/V ERGE (Ex-JOERG N) is one of eight multi-purpose dry-cargo sister ships, initially commissioned and owned by a German Consortium. It was designed by a German design firm, ABH (ABH Ingenieur Technik GmbH) and was built by the Chinese shipyard Weihai Donghai. The 7241 DWT dry-cargo ship M/V ERGE underwent a series of full-scale sea trials in 2010 before it was delivered. Following her build, the initial sea trials were conducted in the Yellow Sea of China on February 5th and 6th, 2010. The sea trial campaign included measurements of ship speed, shaft power, hull performance, and manoeuvring tests. The weather-related environmental conditions during the sea trials are provided in Table 3. In 2023, another set of sea trial was conducted on January 23rd before replacing the CRS (Fig. 3 a) with the GRS (Fig. 3 b). Subsequently, the ship was docked to retrofit the GRS, and the hull was cleaned and painted. A one-component antifouling coating, Jotun SeaQuantum Ultra S, was applied in the drydock before the sea trials with the GRS. It is also known that the same coating was used during the ship's previous drydock with the CRS in 2021, but the coating type for the newly built ship is unknown. This was followed by further sea trials with the retrofitted GRS on May 1st, 2023, which were conducted under the same loading conditions as the ship with the CRS. Sea trials within the GATERS (2021) project were conducted in the Marmara Sea of Türkiye before and after the GRS retrofit for several reasons, including the location of the shipyard, marine traffic, wind and wave conditions, and water depth.

The dedicated sea trials in 2023 included speed-powering trials at varying engine loads as well as the circle manoeuvring and zig-zag tests. An anemometer on a foremast in the bow of the ship measured and recorded the relative wind directions and the wind speed, and a wave buoy was deployed in the sea trials area to obtain significant wave height and average wave period. Shaft speed (n) and torque (Q) measurements to obtain the delivered power ( $P_D$ ), ship location through a GPS device, and fuel consumption through flowmeters were recorded and monitored in real-time during the sea trials. The results obtained by conducting sea trials were corrected in accordance with ISO 15016 (ISO, 2015), taking into account the weather conditions, wind, and waves. The weather conditions were windy, with Beaufort 3 to 4, in the 2023 sea trials with the CRS. Sea trials with the GRS on May 1st, 2023, were conducted in calm water less than Beaufort 2, and hence, no corrections were applied to the measurements.

The dedicated sea trials in 2023 included speed-powering trials at varying engine loads as well as the circle manoeuvring and zig-zag tests. An anemometer on a foremast in the bow of the ship measured and recorded the relative wind directions and the wind speed, and a wave buoy was deployed in the sea trials area to obtain significant wave height and average wave period. Shaft speed (n) and torque (Q) measurements to obtain the delivered power ( $P_D$ ), ship location through a GPS device, and fuel consumption through flowmeters were recorded and monitored in real-time during the sea trials. The results obtained by conducting sea trials were corrected in accordance with ISO 15016 (ISO, 2015), taking into account the weather conditions, wind, and waves. The weather conditions were windy, with Beaufort 3 to 4, in the 2023 sea trials with the CRS. Sea trials with the GRS on May 1st, 2023, were conducted in calm water less than Beaufort 2, and hence, no corrections were applied to the measurements.

**Table 3**  
Environmental conditions in the 2010 sea trials with the CRS.

Parameters	Information
Location	Yellow sea
Weather	Fine
Wave condition	Douglas 3
Air pressure	1020 mbar
Air temperature	2 °C
Water temperature	4 °C

#### 3.1. Hull roughness measurements

Hull roughness measurements were conducted before and after the GRS retrofit in the drydock in 2023 to assess the ageing effect on the performance, as the ship was not new when it was retrofitted with GRS. The roughness measurements conducted at the 120 positions, 60 stations on the flat bottom and 60 stations on the side of the hull, using a handheld stylus-based hull roughness analyser (TQC) were thoroughly assessed to accurately report the hull roughness survey (Ravenna et al., 2023). One traverse of the head of the measurement device at any point on the hull collects information from 10 samples with a traverse length of 50 cm and a sampling interval of 50 mm (Fig. 4). For each 50 mm sample; the microprocessor assesses the mean gradient, known as  $R_{t50}$ , through the peaks and valleys to give the sample's highest peak to lowest valley measurements. The average hull roughness (AHR) of M/V ERGE was calculated as 300  $\mu\text{m}$  both before and after the retrofit, using the mean hull roughness (MHR) measurements based on Eq. (8). The reason for such high-grade hull roughness measurements before and after the GRS retrofit was that the ship's hull was not shot-blasted during the three coating campaigns over the 13 years. As a result, the accumulation of old fouling deposits was not properly removed, leading to considerable hull roughness. It should be noted that most of the measurements were consistent with the average hull roughness, as expected. However, in typical niche fouling areas, such as surfaces around intake or outflow openings, extreme roughness readings were observed, likely due to old fouling deposits. In parallel with the measurements, the increase in hull surface roughness was initially assumed to be approximately 20  $\mu\text{m}/\text{year}$  due to the ageing effect. As a rule of thumb, every 20  $\mu\text{m}$  of hull roughness adds 1% to the required propulsion power (Townsin, 1985). In the study, it was presumed that the hull surface roughness was 120–150  $\mu\text{m}$  when the ship was newly built, with an approximate increase of 12–15  $\mu\text{m}/\text{year}$ , considering the time since the vessel's construction and the measurements. In this context, the discrepancy between the initial assumption and the findings on the annual increment is acceptable, given the uncertainties in the assumptions and, to a lesser extent, in the measurements.

$$\text{MHR} = \frac{1}{10} \sum_{i=1}^{10} R_{t50i}, \text{AHR} = \frac{1}{120} \sum_{j=1}^{120} (\text{MHR})_j \quad (8)$$

#### 3.2. Evaluation of ageing and fouling effect

The above-mentioned sea trials and hull roughness measurements revealed that, for a fair powering performance comparison of the ship with the CRS and GRS configurations, the impact of ageing and fouling should be considered by analysing the results based on the sea trials conducted when the vessel was new in 2010 and just before the GRS was retrofitted in January 2023. Regarding the hull roughness and fouling condition range described by Schultz (2007), the authors agreed that, during the sea trials conducted in 2010, the ship with the CRS had a typical anti-fouling (AF) coating applied. In powering prediction/extrapolation based on the model-scale experiment results, the total resistance coefficient ( $C_{TS}$ ) is calculated using the following Eq. (9).

$$C_{TS} = (1 + k)C_{FS} + \Delta C_F + C_A + C_R + C_{AAS} \quad (9)$$

where  $\Delta C_F$  is the roughness allowance, Eq. (10), as defined below in ITTC (2017c).

$$\Delta C_F = 0.044 \left[ \left( \frac{k_s}{L_{WL}} \right)^{\frac{1}{3}} - 10\text{Re}^{-\frac{1}{3}} \right] + 0.000125 \quad (10)$$

In this study,  $\Delta C_F$  values were either calculated using the standard value of 150  $\mu\text{m}$  (ITTC, 2017c) for the roughness of hull surface ( $k_s$ ), using the average hull roughness (AHR) measurements where  $k_s = 300 \mu\text{m}$ , or read off from the fouling-related practical added resistance diagrams

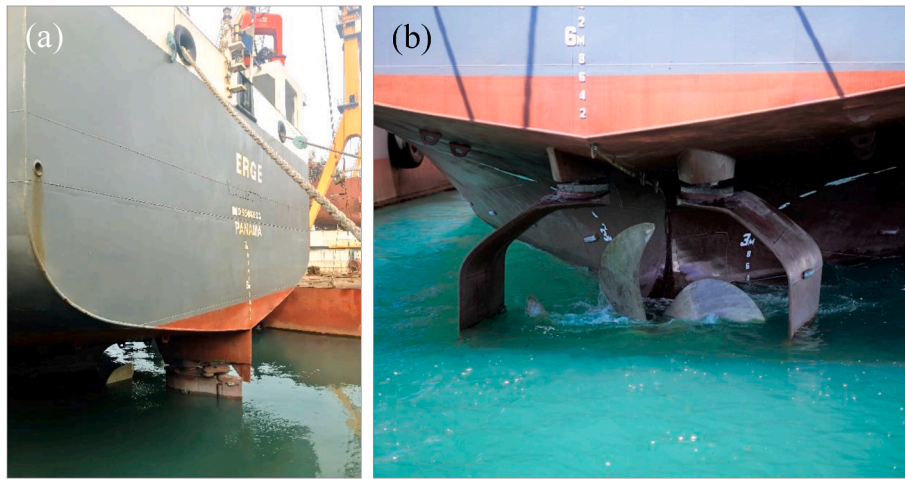


Fig. 3. 7241 DWT multi-purpose dry-cargo ship, M/V ERGE, (a) before and (b) after the GRS retrofit.

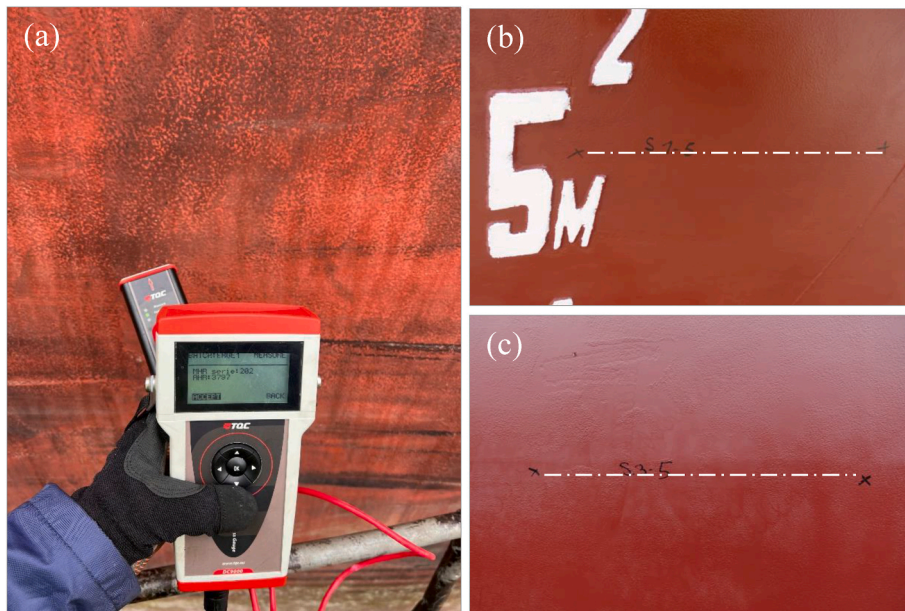


Fig. 4. Hull roughness survey of M/V ERGE, representation of the sampling lines (white dotted dash line) with a length of 50 cm and a sampling interval of 50 mm. (a) Before the GRS retrofit. (b) and (c) After the GRS retrofit.

that were systematically generated by Demirel et al. (2019) based on Schultz (2007) for varying ship lengths and speeds. As presented and discussed in the following section (i.e., Section 4), sea trials power-speed results when the ship was new (in 2010) were found to be consistent with the extrapolated results from the model tests by using  $\Delta C_F$ , estimated from the added resistance diagram as ‘typical for an AF coating’ condition. Furthermore,  $\Delta C_F$ , covering a range of representative fouling scenarios, given by Schultz (2007), was also used to calculate the powering predictions for each fouling scenario within the range. Then, the results were plotted against the sea trials data to determine the fouling condition during the sea trials conducted in 2023. This enabled the authors to align the sea trials results of the ship with the CRS in 2023 with the sea trials in the same condition, but the GRS retrofitted.

#### 4. Results and discussions

Using the above-outlined procedure, the delivered power of M/V ERGE with the CRS and GRS configurations was extrapolated to full-scale from the model test results and plotted in Fig. 5 (a). As shown in

this figure, the GRS significantly reduced the power requirement of the ship at the same speed. The corrected sea trial measurements (GATERS, 2024) analysed according to the ISO 15016 procedure for the ship with the CRS in 2010 and 2023 are also depicted in Fig. 5 (a), along with the trial measurements in 2023 for the GRS. It can be observed in Fig. 5 (a) that the speed range of the sea trials in 2010, which was conducted in the China Sea when the vessel was new, deviates from those conducted in 2023, mainly due to 13 years of ageing and short-term fouling. In order to remedy the situation, initially, an overlapping speed of 11.5 knots could be suggested to enable further analysis of the trial data, as shown in Fig. 5 (b). The results were then slightly extrapolated to reach this overlapping ship speed in both sea trials. The increase in delivered power,  $\Delta P_D$ , was calculated to be 21% between 2010 and 2023 in the CRS configuration, as can be seen in Fig. 5 (b). Using this evaluation, in the following, a practical methodology is proposed to elucidate the reason behind the difference between those sea trials conducted literally for the same ship and the loading condition but to take into account the ageing and fouling state of the ship in 2023 for M/V ERGE with the CRS configuration.

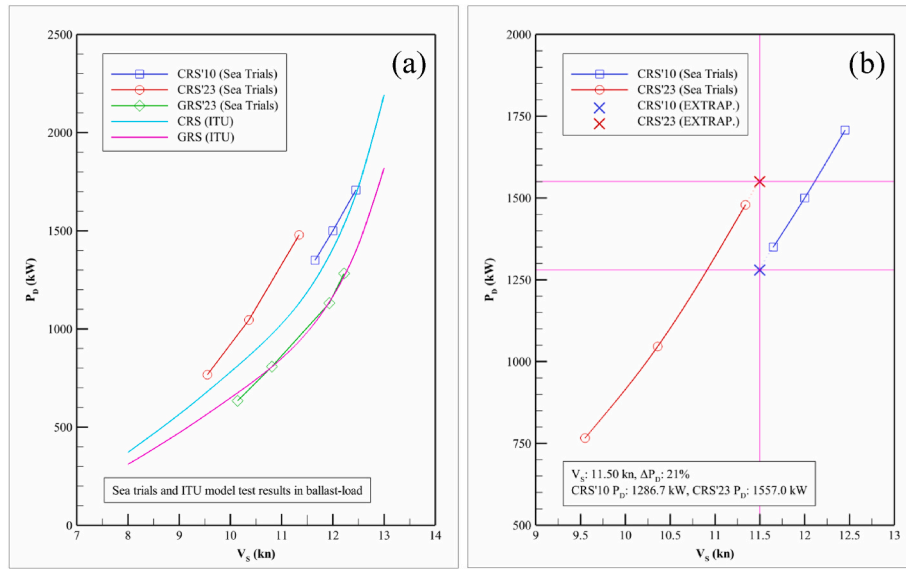


Fig. 5. (a) Comparison of sea trials and model test results extrapolated to full scale by ITTC (2017c) with  $k_s = 150 \mu m$ , using Eq. (9) and Eq. (10). (b) A feasible common speed of sea trial data extrapolation for 2010 and 2023.

As described earlier in Section 3.2, the roughness allowance ( $\Delta C_F$ ) values were extracted using the practical added resistance diagrams for various representative coating and fouling conditions, as shown in Fig. 6 (a). Schultz (2007) proposed these conditions, which included skin friction data of flat plates covered sequentially with a typical AF coating, deteriorated coating or light slime, heavy slime, small calcareous fouling or weed, medium calcareous fouling, medium calcareous fouling, and heavy calcareous fouling.

The 2010 sea trial results of the newly built ship align with the extrapolated results from model tests -assuming the average hull roughness is approximately  $150 \mu m$  (ITTC, 2017c)- as shown in Fig. 5 (a), and using the  $\Delta C_F$  data derived from the practical added resistance diagram under the assumption of 'typical AF coating' as shown in Fig. 6 (b). The delivered power results shown in Fig. 6 (b) were obtained by applying the extracted  $\Delta C_F$  values, using added resistance diagrams for the representative coating and fouling conditions depicted in Fig. 6 (a), into Eq. (9).

In Fig. 6 (b), while the magenta-diamond symbol (◆) corresponds to the predicted delivered power of the ship, with  $\Delta C_F$  for 'typical AF coating', which aligns with the sea trial power data from 2010, the cyan-right-triangle symbol (▶) corresponds to the predicted power with  $\Delta C_F$  for 'heavy slime' condition. From the latter, it can be inferred that the sea trials of the ship with the CRS were conducted under medium to heavy slime fouling conditions in 2023. The underwater and drydock fouling surveys conducted before the GRS retrofit support these findings, as shown in Fig. (7).

The predicted power results for the ship with the CRS under the representative fouling conditions are also shown in Fig. (8), where the dashed black line represents the predicted results based on the model tests and  $\Delta C_F$  calculated from Eq. (10) as defined in the ITTC (2017 c) for further supporting information. The magenta line presents the predicted results with  $\Delta C_F$  for the representative of the typical AF coating from the practical added resistance diagrams. Both sets of results -using the standard value of  $k_s = 150 \mu m$  (ITTC, 2017 c) and the 'typical for an AF

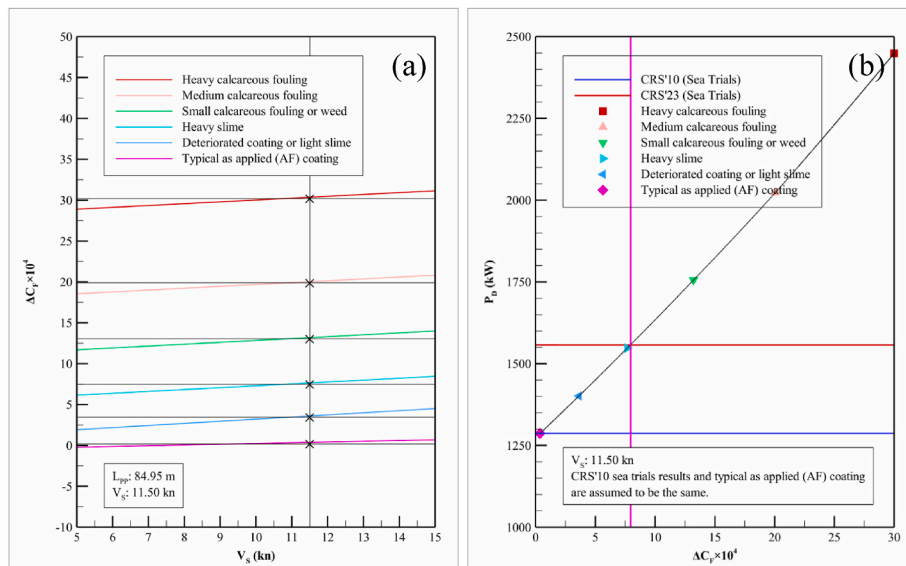


Fig. 6. (a)  $\Delta C_F$  values extracted using the added resistance diagrams. (b) Sea trials and predicted delivered power results based on the representative coating and fouling conditions at 11.5 knots (Fig. 6, a) and Eq. (9).

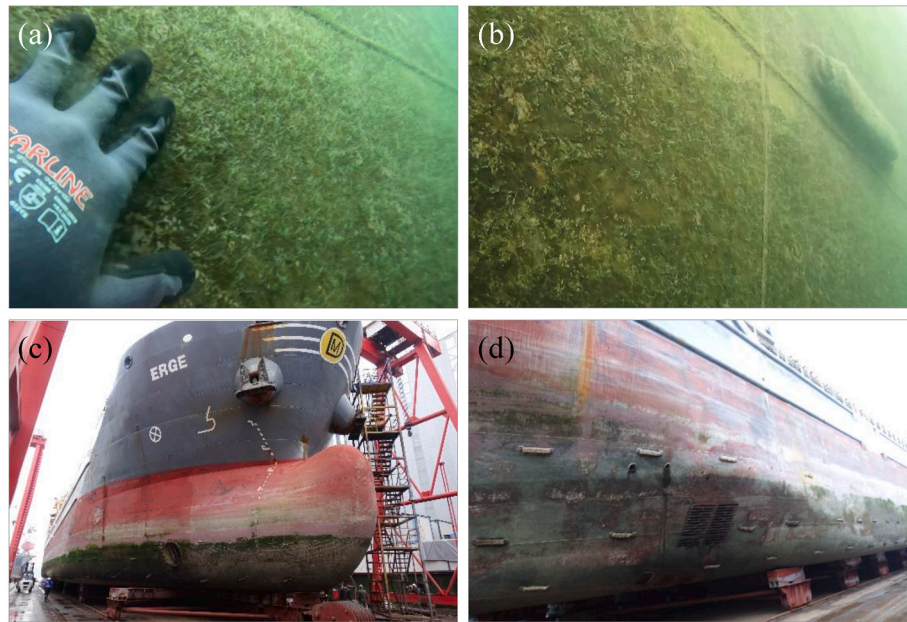


Fig. 7. Images taken during the fouling survey. (a) and (b) underwater, and (c) and (d) in drydock.

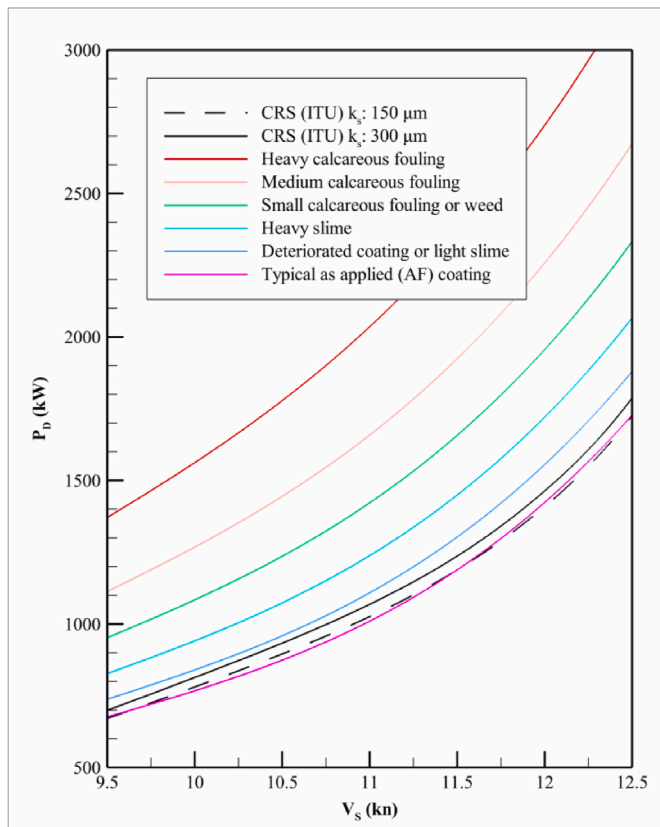


Fig. 8. Predicted delivered power ( $P_D$ ) results according to the representative fouling conditions.

coating' assumption based on added resistance diagrams to determine  $\Delta C_F$  and, consequently,  $C_{TS}$ - align well with each other.

The sea trial results of the ship with the CRS configuration in 2023 were reproduced, considering M/V ERGE's fouling condition in 2023 trials, which was represented by the medium to heavy slime condition

(Fig. 9, a). The results of the GRS retrofitted ship were also reproduced (Fig. 9, a) based on the outcome of the hull roughness measurements before and after the retrofitting, which were almost similar, indicating an average hull roughness  $k_s = 300 \mu$ m. As elaborated earlier in Section 3.1, the reason for such high-grade hull roughness before and after the GRS retrofit was that the ship's hull was not shot-blasted during the three coating campaigns over the 13 years. A comparison of the sea trials in their raw and reproduced forms with the model tests is provided in Table 4 and illustrated in Fig. (9).

The above approach provides a consistent comparison between the sea trials and the extrapolated results obtained by the model tests. As shown in Fig. 9 (b), the ship retrofitted with the GRS exhibited significantly reduced delivered power demand, up to 25%, corroborated not only by the towing tank experiments and numerical analysis but also obtained by the sea trial measurements.

As a summary of this study, the hull condition was initially assessed quantitatively, based on the results of the sea trials in 2010 and 2023 with the CRS, using the model test results and the added resistance diagrams to interpret the differences between those sea trials. The hull fouling surveys, both underwater and in drydock, supported the finding that the sea trials in 2023 with the CRS were conducted under medium to heavy slime fouling conditions, which can be considered a qualitative assessment of the hull condition. The hull was cleaned before the GRS retrofit but was subject to the effects of ageing in the sea trials with the GRS. The hull roughness measurements taken in drydock supported the general assumption regarding the annual increase in surface roughness, considering the time since the vessel's construction and the sea trials with the GRS. The average hull surface roughness value obtained by the measurements was used to reproduce the sea trials with the GRS and compare the results with the model test results extrapolated to full scale. These comparisons were made using either the standard value of 150  $\mu$ m for  $k_s$  or by applying the 'typical AF coating' assumption based on the fouling-related added resistance diagrams. The results were almost the same because both assumptions relate to the hull conditions of newly built ships, leading to identical  $\Delta C_F$  values. Table 5 provides a summary of the sea trials, including hull conditions observed in the trials, based on both quantitative and qualitative assessments, as well as the assumptions made.

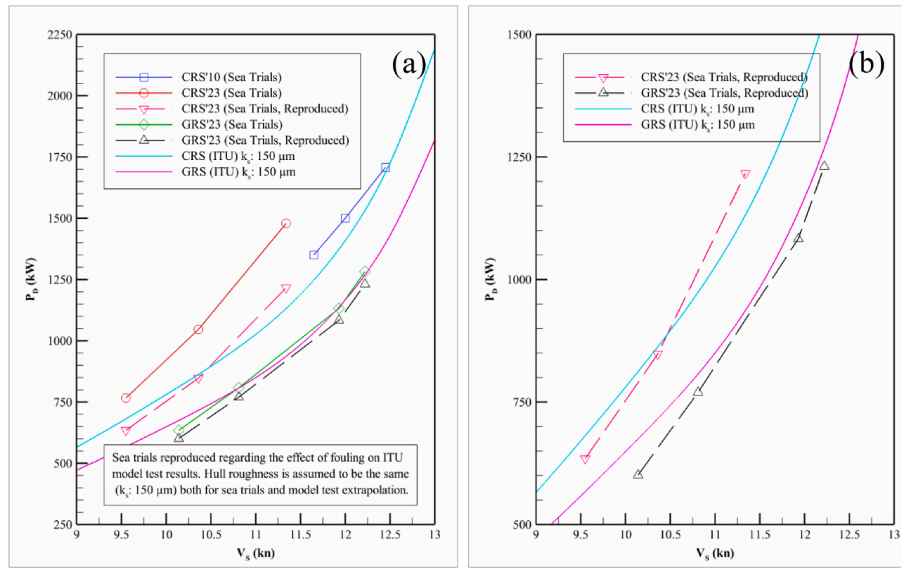


Fig. 9. (a) A comparison of delivered power ( $P_D$ ) obtained by the sea trials in their raw and reproduced forms with the model tests. (b) A comparison of  $P_D$  obtained by the sea trials was conducted in the GATERS project in their reproduced forms.

Table 4

A comparison of  $P_D$  obtained by sea trials in their raw (CRS'10, CRS'23, GRS'23) and reproduced (CRS'23<sub>RP</sub>, GRS'23<sub>RP</sub>) forms with the model tests (CRS, GRS) at  $V_s = 11.5$  knots.

Sea Trials	CRS'10	CRS'23	CRS'23 <sub>RP</sub>	CRS	GRS'23	GRS'23 <sub>RP</sub>	GRS
$P_D$ (kW)	1287	1557	1288	1189	1001	958	984

Table 5

A summary of the sea trails, including hull conditions observed in the trials, based on both quantitative and qualitative assessments, as well as the assumptions made (GATERS, 2024).

Sea Trials	CRS (2010)	CRS (2023)	GRS (2023)
Location	Yellow sea	Marmara sea	Marmara sea
Weather	Fine	Windy	Fine
Wave condition	Douglas 3	Beaufort 3 to 4	Beaufort 2
Hull roughness (AHR)	150 $\mu\text{m}$	300 $\mu\text{m}$	300 $\mu\text{m}$
Fouling condition	No fouling	Medium to heavy	No fouling

## 5. Conclusions

As part of the EU-H2020 GATERS project activities, a detailed analysis of the power-speed performance of the project target ship, M/V ERGE, with her two different rudder systems (i.e., CRS and GRS) was conducted using the results of the towing tank tests and sea trial measurements with particular emphasis on her hull condition due to ageing and fouling effects. The analysis used a practical approach to assess the impact of the hull coating and fouling condition for M/V ERGE with the CRS to ensure a consistent comparison of results under standardised testing conditions.

The approach used involved the powering performance analyses of the data from the ship's trials conducted when the ship with the CRS was new in 2010 and later before and after she was retrofitted with the GRS in January and May 2023, respectively. The effect of the coating and fouling conditions of the hull in 2010 and 2023 was analysed using the extrapolation of the model test results and relatively recent practical fouling-related data provided by Schultz (2007).

These analyses revealed that M/V ERGE with the CRS in January 2023 trials suffered a 21% power increase (at 11.5 knots) due to her 13 years of ageing and temporary medium to heavy slime fouling conditions. The inspection of the hull and roughness measurements after the

January 2023 trials also confirmed the ageing effect by the measured 300  $\mu\text{m}$  average hull roughness.

Following the retrofit of the vessel with the GRS, and based on the further hull roughness measurements after the retrofit, the performance of M/V ERGE was improved by a remarkable 25% power saving based on the comparative trial results in January and May 2023 corrected for weather and fouling conditions. These analyses also indicated that the Gate Rudder System is the major new contender for the most effective energy-saving device (ESD) for ships, not only for new ships but also for existing ships as a retrofit.

## CRedit authorship contribution statement

**Çağatay Sabri Köksal:** Writing – original draft, Validation, Methodology, Investigation, Formal analysis, Data curation, Conceptualization. **Cihad Çelik:** Writing – original draft, Validation, Methodology, Investigation, Formal analysis, Data curation. **Selahattin Özsayan:** Writing – original draft, Validation, Methodology, Investigation, Formal analysis, Data curation. **Emin Korkut:** Writing – review & editing, Supervision, Resources, Funding acquisition. **Mehmet Atlar:** Writing – review & editing, Resources, Project administration, Funding acquisition.

## Declaration of competing interest

The authors declare that they have no known competing financial interests or personal relationships that could have appeared to influence the work reported in this paper.

## Acknowledgements

This paper is based on the activities conducted in the collaborative European project GATERS, which was an Innovation Action Project funded by the EC H2020 Programme (ID: 860337) with independent

aims and objectives. The project had an official sub-license agreement with Wartsila Netherlands BV to utilise the Gate Rudder Patent (EP 3103715) at specific retrofit projects of vessel sizes below 15000 DWT.

## References

- Atlar, M., Aktas, B., Gurkan, A., Sasaki, M., Sun, X., Korkut, E., Felli, M., 2023. The GATERS Project—An innovative way of retrofitting ships for greener and safer operations. *Transport. Res. Procedia* 72, 1958–1965, 2023.
- Bulten, N., 2024. Upgraded MMG-methodology to capture gate-rudder performance aspects. Eighth International Symposium on Marine Propulsors, Smp'24, Berlin, Germany. <https://10.15480/882.9324>.
- Carchen, A., Turkmen, S., Piaggio, B., Shi, W., Sasaki, N., Atlar, M., 2021. Investigation of the manoeuvrability characteristics of a Gate Rudder system using numerical, experimental, and full-scale techniques. *Appl. Ocean Res.* 106, 102419. <https://doi.org/10.1016/j.apor.2020.102419>.
- Çelik, C., Özsayan, S., Köksal, Ç.S., Danişman, D.B., Korkut, E., Gören, Ö., 2022. On the full-scale powering extrapolation of ships with gate rudder system (GRS). In: A. Yücel Odabaşı Colloquium Series 4th International Meeting-Ship Design & Optimization and Energy Efficient Devices for Fuel Economy. Istanbul, Türkiye.
- Çelik, C., Özsayan, S., Köksal, Ç.S., Danişman, D.B., Korkut, E., Gören, Ö., Atlar, M., 2023. On the evaluation of the model test extrapolation by sea trial measurements. In: 7th International Conference on Advanced Model Measurement Technology for the Maritime Industry. Istanbul, Türkiye.
- Demirel, Y.K., Song, S., Turan, O., Incecik, A., 2019. Practical added resistance diagrams to predict fouling impact on ship performance. *J. Sound Vib.* 186. <https://doi.org/10.1016/j.oceaneng.2019.106112>.
- Fukazawa, M., Turkmen, S., Marino, A., Sasaki, N., November, 2018. Full-scale gate rudder performance obtained from voyage data. In: Proceedings of the A. Yücel Odabaşı Colloquium Series: 3rd International Meeting-Progress in Propeller Cavitation and its Consequences: Experimental and Computational Methods for Predictions. Istanbul, Turkey, pp. 15–16.
- GATERS, 2021. Gate rudder system as a retrofit for the next generation propulsion and Steering of ships. The EC - H2020 Project GATERS (Project ID: 860337). <https://10.3030/860337>.
- GATERS, 2024. Gate rudder system as a retrofit for the next generation propulsion and Steering of ships. Full-Scale Trials and Voyage Monitoring of the Target Ship in Task 2.1. The EC - H2020 Project GATERS (Project ID: 860337, 2021). Work Package 2.
- Gürkan, A.Y., Köksal, Ç.S., Aktas, B., Ünal, U.O., Atlar, M., Sasaki, N., 2023c. Computational investigation of the impact of a gate rudder system on A high block coefficient coastal vessel as A retrofit. In: 7th International Conference on Advanced Model Measurement Technology for the Maritime Industry. Istanbul, Türkiye.
- Gürkan, A.Y., Ünal, U.O., Aktas, B., Atlar, M., 2023a. An investigation into the gate rudder system design for propulsive performance using design of experiment method. *Ship Technol. Res.* 71 (2), 199–212. <https://doi.org/10.1080/09377255.2023.2248721>.
- Gürkan, A.Y., Ünal, U.O., Aktas, B., Köksal, Ç.S., Atlar, M., 2023b. Comprehensive investigation of the form design of the gate rudder for propulsive performance using design of experiment method. 25th Numerical Towing Tank Symposium (NuTTS), Ericeira, Portugal.
- Gürkan, A.Y., Turkmen, S., Sasaki, N., Aktas, B., Köksal, Ç.S., Atlar, M., 2023d. Manoeuvrability improvement investigation of a coastal vessel retrofitted with A gate rudder system using computational and experimental methods. In: 7th International Conference on Advanced Model Measurement Technology for the Maritime Industry. Istanbul, Türkiye.
- ISO, 2015. Ships and Marine Technology D Guidelines for the Assessment of Speed and Power Performance by Analysis of Speed Trial Data.
- ITTC, 2017a. ITTC resistance committee. Proceedings of the 28th International Towing Tank Conference, Recommended Procedures and Guidelines, Ship Models 7, 5-01-01-01.
- ITTC, 2017b. ITTC propulsion committee. In: Proceedings of the 28th International Towing Tank Conference. Recommended Procedures and Guidelines, Propulsion/Bollard Pull Test, 7.5-02-03-01.1.
- ITTC, 2017c. ITTC Propulsion committee. In: Proceedings of the 28th International Towing Tank Conference, Recommended Procedures and Guidelines, 1978 ITTC Performance Prediction Method, 7.5-02-03-01.4.
- Köksal, Ç.S., Aktas, B., Gürkan, A.Y., Korkut, E., Sasaki, N., Atlar, M., 2022. Experimental powering performance analysis of M/V ERGE in calm water and waves. In: A. Yücel Odabaşı Colloquium Series 4th International Meeting-Ship Design & Optimization and Energy Efficient Devices for Fuel Economy. Istanbul, Türkiye.
- Köksal, Ç.S., Gürkan, A.Y., Aktas, B., Ünal, U.O., Fitzsimmons, P., Sasaki, N., Atlar, M., 2023a. Cavitation Observation of M/V ERGE during the Sea Trials: a comparison of gate rudder and conventional rudder configurations. In: 7th International Conference on Advanced Model Measurement Technology for the Maritime Industry. Istanbul, Türkiye.
- Köksal, Ç.S., Gürkan, A.Y., Aktas, B., Turkmen, S., Zoet, P., Sasaki, N., Atlar, M., 2023b. Underwater radiated noise measurements of Pre-and Post-retrofit of gate rudder system during the Sea Trials. In: 7th International Conference on Advanced Model Measurement Technology for the Maritime Industry. Istanbul, Türkiye.
- Köksal, Ç.S., Gürkan, A.Y., Aktas, B., Sasaki, N., Atlar, M., 2023c. Influence of gate rudder system (GRS) rudder angle(s) on the propulsive efficiency. 25th Numerical Towing Tank Symposium (NuTTS). Ericeira, Portugal.
- Köksal, Ç.S., Gürkan, A.Y., Aktas, B., Sasaki, N., Atlar, M., 2024a. Experimental assessment of hull, propeller, and the gate rudder system interaction in calm water and oblique waves. *Ocean Engineering*. <https://doi.org/10.1016/j.oceaneng.2024.119144>.
- Köksal, Ç.S., Gürkan, A.Y., Aktas, B., Ünal, U.O., Fitzsimmons, P., Sasaki, N., Atlar, M., 2024b. Quantifying the influence of Gate Rudder System (GRS) rudder angle (s) on propeller cavitation. In: 8th International Symposium on Marine Propulsors, Smp 2024, Berlin, Germany. <https://10.15480/882.9364>.
- Mizzi, K., Zammit Munro, M., Gürkan, A.Y., Aktas, B., Atlar, M., Sasaki, N., 2022. The performance prediction and energy saving evaluation for the retrofit of a gate rudder system on a general cargo vessel using CFD procedures. In: A. Yücel Odabaşı Colloquium Series 4th International Meeting-Ship Design & Optimization and Energy Efficient Devices for Fuel Economy. Istanbul, Turkey.
- Özsayan, S., Aydın, Ç., Köksal, Ç.S., Ünal, U.O., Korkut, E., 2023. Effects of the gate rudder system (GRS) on the experimental cavitation Observations and noise measurements. In: 7th International Conference on Advanced Model Measurement Technology for the Maritime Industry. Istanbul, Türkiye.
- Özsayan, S., Aydın, Ç., Köksal, Ç.S., Ünal, U.O., Korkut, E., 2024. Assessment of the gate rudder system on the cavitation and underwater radiated noise characteristics of a containership. *Ocean Engineering*. <https://doi.org/10.1016/j.oceaneng.2024.119391>.
- Ravenna, R., Özsayan, S., Köksal, Ç.S., Atlar, M., 2023. M/V ERGE's Hull Fouling and Roughness Survey Report. The EC - H2020 Project GATERS. Project ID: 860337, 2021).
- Santic, I., Mauro, S., Micci, G., Felli, M., 2023. Systematic experimental survey of propulsive and Acoustic performances of a gate rudder system in relation to a conventional rudder. In: 7th International Conference on Advanced Model Measurement Technology for the Maritime Industry. Istanbul, Türkiye.
- Sasaki, N., Atlar, M., 2018. Investigation into the propulsive efficiency characteristics of a ship with the Gate Rudder propulsion. In: A. Yücel Odabaşı Colloquium Series:3rd International Meeting on Progress in Propeller Cavitation and its Consequences: Experimental and Computational Methods for Predictions. November.
- Sasaki, N., Atlar, M., 2024. Gate rudder system and ship design. Eighth International Symposium on Marine Propulsors, Smp'24, Berlin, Germany. <https://10.15480/882.9301>.
- Sasaki, N., Atlar, M., Kuribayashi, S., 2016. Advantages of twin rudder system with asymmetric wing section aside a propeller: the new hull form with twin rudders utilising duct effects. *J. Mar. Sci. Technol.* 21, 297–308. <https://doi.org/10.1007/s00773-015-0352-z>.
- Sasaki, N., Kuribayashi, S., Asaumi, N., Fukazawa, M., Nonaka, T., Turkmen, S., Atlar, M., October, 2017. Measurement and calculation of gate rudder performance. In: The 5th International Conference on Advanced Model Measurement Technology for the Maritime Industry.
- Sasaki, N., Kuribayashi, S., Miles, A., 2019. Full Scale Performance of Gate Rudder. Royal Institution of Naval Architects (RINA)-Propellers and Impellers: Research, Design, Construction and Application, London, UK. <https://doi.org/10.3940/rina.pro.2019.10>.
- Sasaki, N., 2022. Private Communications on Powering Aspects of Ships with GRS.
- Schultz, M.P., 2007. Effects of coating roughness and biofouling on ship resistance and powering. *Biofouling* 23 (5), 331–341. <https://doi.org/10.1080/08927010701461974>.
- Tacar, Z., Sasaki, N., Atlar, M., Korkut, E., 2020. An investigation into effects of Gate Rudder® system on ship performance as a novel energy-saving and manoeuvring device. *Ocean Engineering* 218, 108250. <https://doi.org/10.1016/j.oceaneng.2020.108250>.
- Townsin, R.L., 1985. The ITTC Line-Its Genesis and Correlation Allowance. The Naval Architect, London, UK.
- Turkmen, S., Carchen, A., Sasaki, N., Atlar, M., 2015. A new energy saving twin rudder system-gate rudder. In: SCC 2015 International Conference on Shipping in Changing Climates: Technologies, Operations, Logistics and Policies towards Meeting 2050 Emission Targets.
- Turkmen, S., Fukazawa, M., Sasaki, N., Atlar, M., 2018. Cavitation Tunnel tests and full-scale review of the first gate rudder system installed on the 400TEU container ship. In: A. Yücel Odabaşı Colloquium Series 3rd International Meeting on Progress in Propeller Cavitation and its Consequences: Experimental and Computational Methods for Predictions, pp. 29–39. Istanbul Turkey.